Chemical Engineering Journal 435 (2022) 134881

Contents lists available at ScienceDirect

Chemical Engineering Journal

journal homepage: www.elsevier.com/locate/cej

# Weathering of plastic SODIS containers and the impact of ageing on their lifetime and disinfection efficacy

Ángela García-Gil [a], María Dolores Molina-Ramírez [a], Rafael A. García-Muñoz [a], Ramesh Marasini [b], Lyndon Buck [b], Kevin G. McGuigan [c], Javier Marugán [a,*]

[a] Department of Chemical and Environmental Technology (ESCET), Universidad Rey Juan Carlos, C/ Tulipán s/n, 28933 Móstoles, Madrid, Spain
[b] School of Art, Design and Performance, Buckinghamshire New University, High Wycombe, HP11 2JZ, United Kingdom
[c] Department of Physiology & Medical Physics, RCSI University of Medicine and Health Sciences, Dublin DO2 YN77, Ireland

ARTICLE INFO

*Keywords:*
Solar water disinfection
*E. coli*
Weatherometer
Kinetic modelling
Spectral action
Photostability

ABSTRACT

This work aims to study the ageing of plastic materials suitable for manufacturing solar water disinfection (SODIS) containers, such as PET, polymethylmethacrylate (PMMA), and polypropylene (PP) with and without UV-stabiliser. The evolution of mechanical and optical properties, and disinfection rates were studied over different weathering periods. PMMA and PP with a 1% content by weight of UV-stabiliser were shown to be excellent candidate materials for manufacturing SODIS devices, since they presented stable optical and mechanical properties, and both transmit UVB radiation. Since PMMA is a UV resistant but fragile, easily scratched material with a lifetime above one year, it should be selected for static SODIS devices, while PP with 1% of UV-stabiliser should be chosen for portable devices because of its great resistance and elasticity for up to nine months of solar exposure. Both materials were considered profitable on the basis of their lifetime/costs ratio. PET showed great mechanical properties for one year but, in contrast, suffered of a deterioration of its optical properties and disinfection rates. PP without UV-stabilisers suffered a dramatic degradation after a very short exposure of 2 months. Finally, a kinetic model that considers the radiation spectral distribution (thus, the transmittance spectra of the plastics as a function of the ageing time) is proposed to estimate the required solar exposure time to achieve water disinfection for the proposed plastic SODIS containers. A good agreement between predicted and experimental data was achieved, especially for containers manufactured with PET and both PPs (errors below 25%).

## 1. Introduction

Solar water disinfection (SODIS) is one of the most suitable treatments to produce safe drinking water at the household level [1]. It requires no consumables, and is one of the least expensive treatment (estimated costs of $0.63 per person per year vs $0.66 for chlorination and $3.03 for filtration [2]). SODIS only relies on solar energy, and its effectiveness for the removal of pathogens from water has been widely proven [3,4]. A SODIS guidance [5] was published to encompass a standard procedure for worldwide adoption. Briefly, water with a maximum turbidity level of 30 NTU should be exposed to sunlight in clean polyethylene terephthalate (PET) bottles of 2 L for 6 h on sunny days (48 h on cloudy days), and it is recommended to replace each bottle after 6 months. However, it has been proven that using plastics other than PET can enhance the disinfection efficacy, especially for waters contaminated with viruses and protozoa which can only be photoinactivated by solar UVB radiation [6–8].

Ideally, a SODIS container material should have good optical and mechanical properties and a high durability/cost ratio. Regarding the optical properties, SODIS mainly relies on damage caused to pathogens by solar UV radiation. However, a pathogen's susceptibility varies with the photon wavelength. Thus, the wavelengths transmitted into the interior of SODIS devices is a critical factor for disinfection performance. The transmission spectrum of PET only allows UVA radiation to pass, filtering out the most active wavelengths in the UVB range. Alternative devices and materials transparent to the UVA and UVB radiation [6] have been successfully evaluated, such as polypropylene (PP), polycarbonate (PC), and polystyrene (PS) 1 L bottles [9], polyethylene (PE) bags [10] and polymethylmethacrylate (PMMA) containers [11–13]. Concerning mechanical properties, SODIS containers are usually used to

* Corresponding author.
*E-mail address:* javier.marugan@urjc.es (J. Marugán).

https://doi.org/10.1016/j.cej.2022.134881
Received 1 December 2021; Received in revised form 19 January 2022; Accepted 21 January 2022
Available online 26 January 2022
1385-8947/© 2022 The Author(s). Published by Elsevier B.V. This is an open access article under the CC BY license (http://creativecommons.org/licenses/by/4.0/).

collect, treat, and store the water in order to minimise the risk of recontamination [14]. This is the reason why an ideal SODIS container should be resistant to breakage and deformity, as well as being lightweight, properties that can be guaranteed by different plastics. If the SODIS system is not portable, such as the larger systems used to provide safe drinking water in small schools or clinics [1,12,13], it is not essential to achieve good mechanical properties since the devices are not subjected to falls and scratches [15,16]. Finally, a SODIS container must be economically viable. Production costs and durability vary widely with the type of plastic, and often the price of the most expensive plastics can be offset against durability. Unfortunately, most households do not have the funds required or the only material locally available may not be suitable.

The durability of plastics is closely related to resistance to weathering. The harmful effects of weather exposure on plastics are primarily attributed to photodegradation or photooxidation processes caused by UV light and the action of oxygen [17]. In addition, it is well-known that temperature and humidity accelerate degradation [18,19]. In the context of photostability, plastics can be grouped into: poorly photostable (such as PS, PP, and PE); moderately photostable (such as PET and PC); and highly photostable (such as PMMA) with outdoor half-lives of less than one year, a few years or many years, respectively [20]. Degradation can be attenuated if temperature, UV-light exposure, and contact with oxygen and water, are controlled [21] by avoiding unnecessary thermal exposure, removing oxygen and water contact as much as possible, and adding UV-stabilisers to the plastic during manufacture. However, such mitigation measures are not possible for SODIS containers, since they must necessarily be exposed to the sunlight, which warms them; the container's walls are always in contact with water and oxygen, and the integration of UV-stabilisers may affect the UV transparency, reducing microbicidal efficacy. In addition, the ageing of plastic containers due to weathering can also affect their optical properties, which leads to poorer disinfection rates [22].

Therefore, the selection of new plastic materials for manufacturing SODIS containers must consider not only the initial optical and mechanical properties but also their degradation with increasing solar exposure time. This study aims to investigate the ageing of SODIS container plastic materials exposed to weathering and to find a correlation with the mechanical and optical properties to appraise the effects on the durability of containers and their disinfection rates. Different plastics (PET, PMMA and PP with or without UV-stabiliser) were studied and characterised for SODIS process by using Gel Permeation Chromatography (GPC), Differential Scanning Calorimetry (DSC), and infrared spectroscopy (FTIR). The tensile and flexural properties were obtained using a tensile strength rig and the optical properties were measured by UV–Vis spectroscopy.

## 2. Materials and methods

### 2.1. Ageing test

The ageing of PMMA, PET, and two types of PP from four different current SODIS devices was evaluated:

- PMMA: this plastic is classified as highly photostable and was obtained from static solar reactors used to treat rainwater in South Africa and Uganda [12,13]. This system consisted of a 20 L tubular reactor made with UV-transparent PMMA coupled to an aluminium compound parabolic collector.
- PET: this plastic is classified as moderately photostable and was extracted from transparent 25 L jerrycans used for the solar disinfection of drinking water in rural villages in Mekelle, in Northern Ethiopia [23].
- PP1: this plastic is classified as poorly photostable and was extracted from transparent buckets used in rural villages of Southern Malawi [24,25]. A peculiarity of this PP1 is that it contains 1% by weight of UV-stabiliser.
- PP2: this plastic is classified as poorly photostable and was extracted from transparent 10 L jerrycans manufactured in the UK and planned to be deployed for solar disinfection of water in rural India [26].

Numerous samples of the previous materials were collected and aged by accelerated laboratory weathering tests. The accelerated ageing was carried out according to the standard ISO 4892–2 procedure using the Atlas Weather-Ometer Ci4000. The system was equipped with a xenon lamp and type S borosilicate glass inner and outer filters. This combination is the most common for weathering tests since it reasonably simulates the ultraviolet and visible sunlight region [27]. The samples were exposed to weathering cycles under continuous irradiation with an intensity of 0.75 W/m$^2$ at 340 nm for 8 weeks, corresponding to 3.6 MJ/m$^2$·nm. This radiation dose matches with the annual dose received in Mekelle (4.0 MJ/m$^2$·nm [28] or in Miami (3.0–4.0 MJ/m$^2$·nm [29]). Each cycle has two segments. The first one is a wet phase in which deionised water is sprayed to the front face of the samples for 18 min (simulating raining), and the second one is a dry phase with a relative humidity of 50% that takes 102 min. The air chamber temperature and the black panel thermometer temperature were set at 38 °C and 65 °C, respectively. Samples were collected every week, corresponding to a real equivalent time of one month and a half of ambient exposure. It is worth noting that during the SODIS process, the external surface of the container is always in contact with air, whereas a significant part of the internal surface can be in contact with water. Therefore, this test corresponds to the worst case scenario in which both faces are in contact with oxygen from the air.

### 2.2. Plastics properties measurements

High temperature gel permeation chromatography (HT-GPC) analyses were performed to study the molecular weight of the PP materials for each aged sample. A GPC-IR6 from Polymer Char (CN1952C010) with a GMHH-R precolumn and three PLgel Olexis 3 columns was used to perform the analyses at 150 °C. The columns were calibrated with polystyrene standards, and 1,2-dichlorobenzene was used as the eluent and solvent. The flow rate was 1 mL/min.

Tensile properties for PPs and PET were measured according to a modified ISO527 method. The tensile bars used were type 5A. Before testing, the samples were acclimatised at 23 °C/50% RH for at least 48 h. The samples were tested on an MTS Alliance RT/5 tensile tester. The clamp length was 50 mm, and the test speed 20 mm/min. The percentage elongation and nominal strain at break were also measured, and yield properties were used to estimate Young's modulus with the extensometer. Each sample was tested in triplicate, and the values were averaged. Flexural properties for PMMA were tested on an MTS Insight machine with a 30 kN load capacity. Flexural tests (under three-point bending configuration) were carried out according to a modified ISO178 method. The radius of the two supports and central loading edge was 5.0 mm, and the test speed was 2 mm/min. The difference with the original ISO standard was the dimensions of the used bars, which had a rectangular shape of 10x30 mm, and 3 mm of thickness. The PMMA supplier delivered the samples already cut in this way, which is why the tensile properties of PMMA were measured by impact tests rather than tensile tests. Before testing, the samples were acclimatised at 23 °C/50% RH for at least 48 h. Each sample was tested in triplicate and the values were averaged.

Fourier transform infrared spectroscopy (FTIR) on all the plastics was performed using an FTIR Varian Excalibur Series 3100 spectrometer in attenuated total reflection (ATR) mode for 32 scans. The spectra were collected in the 600–4000 cm$^{-1}$ range, and resolution was 2 cm$^{-1}$. The carbonyl index was calculated from the ratio between the absorbance at 1715 cm$^{-1}$ (maximum point for the carbonyl group) and the absorbance at 974 cm$^{-1}$ for the PMMA and the PPs, and 725 cm$^{-1}$ for the PET (the

absorbance stayed constant at these wavelengths with the weathering). The crystallinity index was calculated for the PPs as the ratio between the absorbance at 998 $cm^{-1}$ (isotactic polypropylene band [30]) and the absorbance at 974 $cm^{-1}$.

Differential scanning calorimetry (DSC) was used to evaluate the thermal properties of the PPs samples of the weeks 0, 2, 4, and 8 using a DSC Mettler-822e. Each sample (8–9 mg) underwent three successive cycles (heating–cooling-heating) under nitrogen from 20 °C (room temperature) to 220 °C at the rate of 10 °C/min.

The optical properties of all the plastic were evaluated by recording their direct transmittance spectra in the UV–Vis range (UVB: 280–320 nm, UVA: 320–400 nm, and Vis: 400–800 nm) with a Vary Carian 500 spectrophotometer. PMMA, PET, and PP1 were found to be very clear plastics in comparison with the translucent PP2. For this reason, also the diffuse transmittance spectrum was measured for PP2.

### 2.3. Disinfection test

An optically differential photoreactor was used to assess the effect of weathering on the disinfection rates. A quartz spectrophotometric cell of 3 mL volume was selected as an optically differential photoreactor to ensure low optical density conditions and neglect radiation profiles, assuming homogeneous radiation intensity throughout its volume. Only one face of the cell (frontal face) was illuminated by the radiation source. The aged plastic samples were located between the illumination source and the frontal face of the photoreactor to simulate that the disinfection reactions were carried out in SODIS devices made with the aged plastics (quartz is totally transparent to the UV–Vis radiation). Sunlight illumination was simulated under controlled conditions with a xenon lamp (Osram XBO 5000 W/H XL) with a temperature colour of 6000 K located on a customised reflector to ensure adequate homogeneous illumination of the water container. The emission spectrum of this lamp matches satisfactorily with the solar spectrum at the Earth surface in the UV range [31]. Irradiance at the surface of the photoreactor was measured by spectroradiometry using a calibrated StellarNet Spectrometer UVIS-25 (329–400 nm). Two sets of experiments were carried out. Firstly, experiments with the original un-aged plastic samples were used to optimise the kinetic model parameters. The second set of experiments were performed with the aged samples (8 experiments per type of plastic) to validate the kinetic model fit. The experiments were carried out at a UV irradiance value of 33.0 ± 2.4 $W/m^2$ at least twice to ensure replicability.

Experiments were carried out with deionised water inoculated with wild *Escherichia coli* sp. as model microorganism. The bacteria were isolated from wastewater from the Rey Juan Carlos university (Móstoles, Spain) sewage plant and inoculated with an initial concentration of $10^6$ CFU/mL. Fresh liquid cultures were prepared by inoculation in Luria-Bertani (LB) nutrient medium and incubation at 37 °C with rotary shaking for 24 h. To prepare the reaction media, 5 mL of the liquid culture were centrifuged at 3000 rpm for 15 min. Bacteria were separated from supernatant, rinsed again with 5 mL of sterile saline solution (NaCl 0.9%), and diluted into the experimental container to obtain the initial concentration. Samples taken during the experiments were analysed using the standard serial dilution method and plating in LB agar, with the colonies counted after incubation for 24 h at 37 °C. The detection limit of this method was 2 CFU/mL. The experimental temperature was always below 30 °C to avoid any thermal effect on the bacteria inactivation.

### 2.4. Kinetic modelling

Inactivation rates were calculated using a multitarget inactivation model proposed by Harm [32] in order to account for the shoulder observed in the majority of the bacteria disinfection curves:

$$\frac{C}{C_o} = 1 - (1 - \exp(-k \cdot t))^m \quad (1)$$

where $C_o$ is the initial bacteria concentration (CFU·$mL^{-1}$), $C$ is the bacteria concentration (CFU·$mL^{-1}$) measured at time $t$ (s), $k$ is the first-order kinetic constant, and $m$ is the shoulder constant.

The values of the observed kinetic constants were obtained minimising the root-mean-square logarithmic error (RMSLE) between the experimental data of the *E. coli* concentration variation with the time (C) and the concentrations estimated with Eq. (1) being $k = k_{obs}$ using the Microsoft Excel solver.

Regarding the procedure to obtain the predicted kinetic constant, the spectral sensitivity of bacteria was taken into account using the procedure developed by Fisher *et al.* [9] for virus inactivation modelling and later applied for bacteria inactivation modelling by Silverman *et al.* [33]. The kinetic constant is defined as a function of the sensitivity coefficients $P(\lambda)$ and the irradiance $E(\lambda)$ for each wavelength. $P(\lambda)$ describes the sensitivity of a microorganism to each wavelength of light and was obtained from the work of Silverman *et al.* [33]. Due to the characteristics of the reactor, the value of $E(\lambda)$ can be assumed constant within the reactor and equal to the irradiance value at the front face. A multiplicative factor ($F$) was included in the expression to fit the global sensitivity of the specific *E. coli* strain but keeping the shape of the spectral sensitivity to the different wavelengths.

$$k_{pre} = F \cdot \int P(\lambda) \cdot E(\lambda) d\lambda \quad (2)$$

$F$ and $m$ were determined using Microsoft Excel solver to minimise the root-mean-square logarithmic error (RMSLE) between predicted and observed bacteria concentration of the disinfection experiments with the original samples (without ageing, week 0). The fit of these parameters was validated with a second set of experiments with the aged plastics. The values of $F$, $m$, and $P(\lambda)$ did not change, but the value of $E(\lambda)$ was recalculated since the transmittance of plastic lowered because of weathering.

## 3. Results and discussion

### 3.1. Accelerated ageing

Pictures of the appearance of the four aged plastics are found in the Supplementary Material (SM) (Fig. S1). Texture changes and increased brittleness were visually observed in all the samples as the ageing process proceeded, except for PMMA. Visually, PET developed a yellowish colour, while PP2 became more translucent. PP1 appeared to be more photostable than PP2, likely because of the presence of 1% of UV-stabiliser in the formulation. In agreement with the literature, PMMA appeared to be a very photostable polymer, in contrast with PET and PP [20].

### 3.2. Mechanical properties

It is well known that flexural and tensile modulus can be used to evaluate the resistance properties of materials. Fig. 1 shows the Young's modulus for PET, PP, and PMMA. For PET and PP Young's moduli were obtained from tensile test data taken from the linear part of the stress–strain curve, while for PMMA flexural tests were used. Both procedures allowed us to obtain the Young's modulus and, thus, to compare the proposed polymers. A high modulus means that specimens can withstand larger stresses at the same strain. Regarding results from Fig. 1, PMMA is clearly the hardest and most rigid material, followed by PET and finally PP1 and PP2 with moderate Young's modulus and high elongation at break for non-degraded samples (Fig. S2), thereby displaying soft but tough behaviour compared to PMMA and PET.

Flexural and tensile strength can also be used to evaluate the

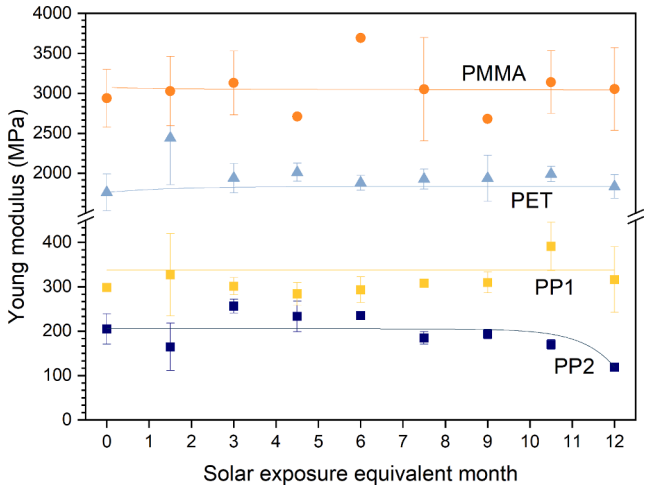


**Fig. 1.** Variation of Young's modulus with the weathering for PMMA, PET, PP1, and PP2. Trendline added only as a visual reference.

resistance of a sample to strain. As long as the plastic material is homogeneous, the tensile strength correlates well with the flexural strength. In addition, most of the materials have small or large defects that concentrate stresses locally which, in turn, provokes localised points of weakness. PMMA samples, whose mechanical properties were measured by flexural test, seemed to be very homogenous (Fig. S1). Considering this, the values of the PMMA properties were compared with those of PET and PP. Fig. 2 shows the variation of the maximum flexural strain before breaking and the corresponding flexural strength for the aged PMMA samples. As can be observed, both properties remained constant with ageing across the studied period, indicating that PMMA is a highly photostable plastic [20] and can be used for long periods (at least for the studied period, equivalent to 1 year on natural conditions). High values of maximum flexural strength and low values of the maximum strain indicate that PMMA is a hard but rigid plastic. In this sense, PMMA would be a good material for a long exposure time of static SODIS devices such as the PMMA large-volume batch solar reactors used in sub-Saharan Africa to treat rainwater [12,13]. Although the material is expensive (28.9€/kg (data from Ecoinvent 2.0 database [34]), the long lifetime offsets this expense. Fig. 2 also shows the variation of tensile strength and the maximum strain (before breaking) for PET, PP1, and PP2. In the case of PET, the tensile strength value decreases slightly in the first months until a constant value was reached. On the other hand, the maximum strain remained stable throughout the exposure time, also leading to excellent durability properties across the equivalent year of exposure. PET proved to be a hard and strong plastic material even after the ageing process, with an adequate ductility, which provides this material with balanced mechanical properties for use in portable SODIS devices. In the case of PP1, the results of the maximum strain assays varied greatly (even for the replicates of the same sample), obtaining low and high values until the last months. This variability is probably caused by the anisotropy and heterogeneicity in the material caused by the addition of the UV-stabiliser. In the case of PP2, maximum

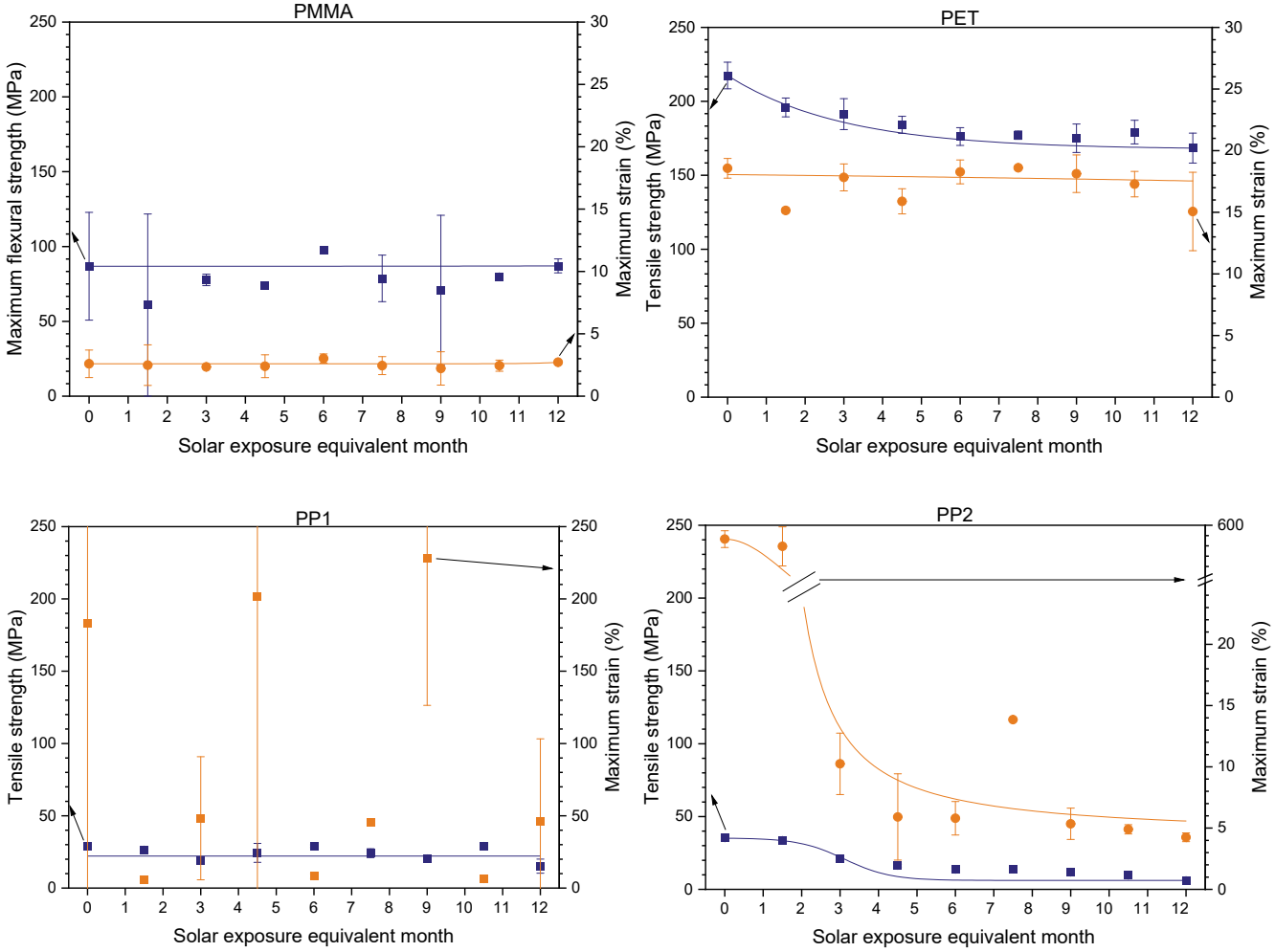


**Fig. 2.** Variation of the tensile and flexural properties with the weathering for PMMA, PET, PP1, and PP2. Trendline added only as a visual reference.

strain decreased dramatically after the second month of exposure. Due to the low values of tensile strength and the sharp declining elongation at break with time (Fig. S2), PP2 proved to be a very brittle plastic material. Therefore, replacements of PP2 devices should be available after only two months because of its high fragility after this period, in which PP2 loses both yield and ductile properties (Fig. S2), making it a far from eco-friendly and cost-effective material.

### 3.3. Thermal and photo oxidation

FTIR spectroscopy is a very effective technique to monitor the influence of different weathering conditions (irradiation, temperature, humidity, or oxygen) on the evolution in chemical structure of polymers. During the exposure of the SODIS polymeric containers, photooxidation and thermal oxidation of the plastics may occur, leading to the formation of molecular defects and an increase in the weakness of the material [35,36].

Carbonyls are one of the most characteristic products of degradation and can be easily monitored by FTIR and evaluated by the carbonyl index. Fig. 3 shows the variation of the carbonyl index for the studied plastics. As can be observed, PMMA maintains the same value during the weathering, while PET only shows a slight decrease, suggesting that neither plastics undergo significant oxidation when they are exposed to the natural environmental conditions for up to one year. These results agree well with those reported in the literature, in which PMMA is defined as highly photostable and PET as a moderate photostable polymer [20]. In contrast, PP is a poorly photostable material, and this is reflected in the results. Fig. 3 shows that the value of the carbonyl index rises for both PPs, indicating that oxidative degradation is occurring. In the case of PP1, oxidation is slower, and this is probably due to the presence of the UV-stabiliser that absorbs a significant part of the radiation responsible for the photooxidation of the PP chains. From the 9th solar equivalent exposure month, the degradation of the plastics takes place probably due to the deterioration of the UV-stabiliser. Therefore, it is recommended to replace it each nine months. However, its low price (8.25€/kg (data from Plastic Europe database [37]) makes PPs SODIS containers with a 1% UV-stabiliser an affordable option.

In order to study the difference between both PP materials, the crystallinity index was also calculated (Fig. 4). For all the aged samples, the crystallinity index of PP2 was higher than that of PP1, which indicates that PP2 possesses more brittleness than PP1. It is also noteworthy to observe the different evolution of the crystallinity index for

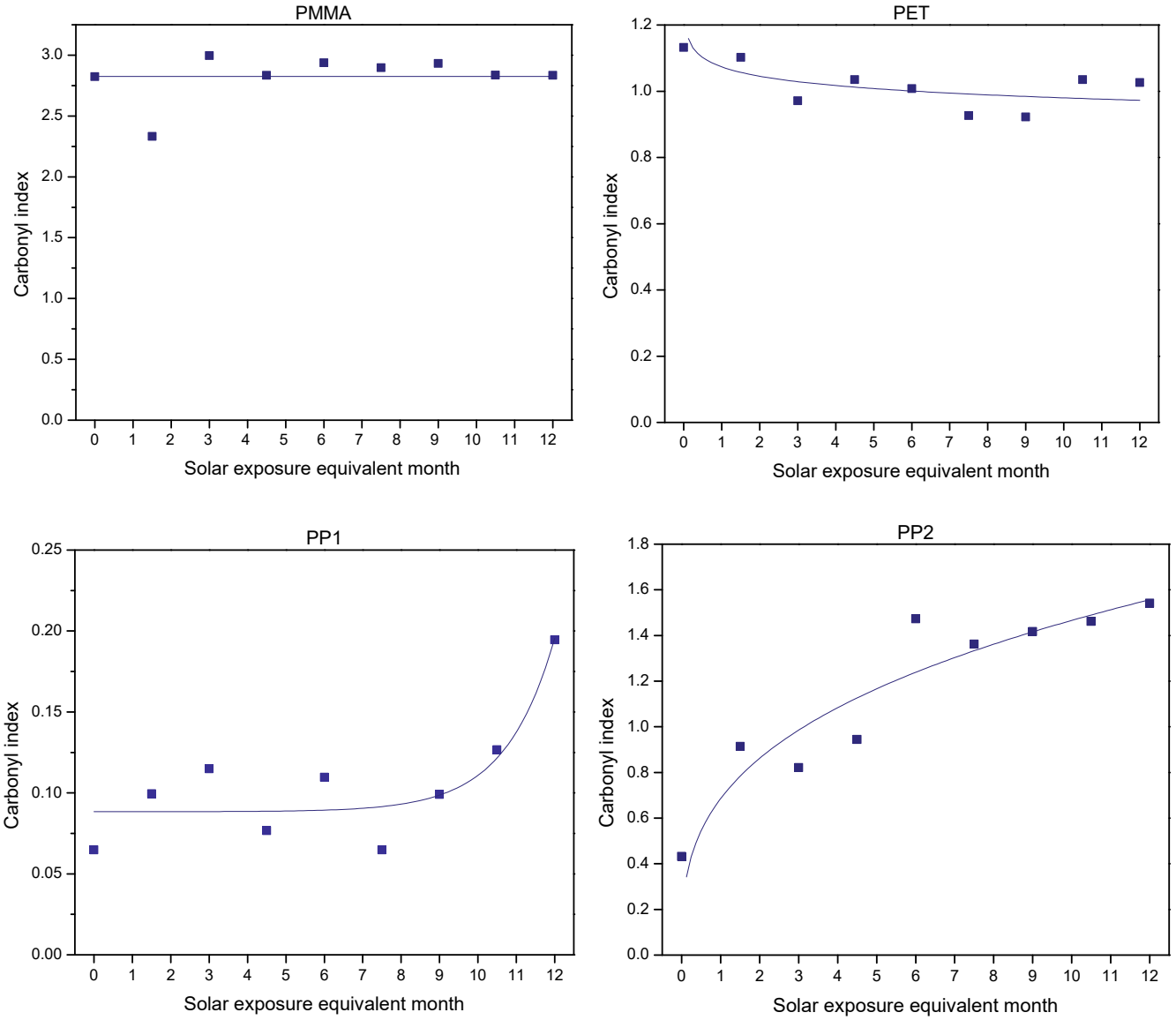


**Fig. 3.** Changes in the carbonyl index during the ageing process. Trendline added only as a visual reference.

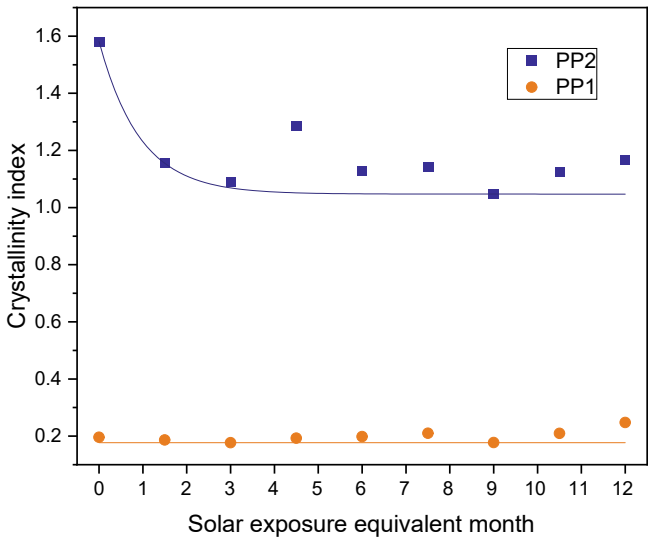


**Fig. 4.** Evolution of the crystallinity index during the ageing process. Trendline added only as a visual reference.

each PP. While the value for PP1 remained stable and low around 0.2 with weathering, the crystallinity index of PP2 experienced a decrease from the first two solar exposure equivalent months, but remained constant after that. The differences in cristallinity between both PPs are readily observed. Fig. S1 shows that the PP1 series are more transparent than PP2, which displays greater opacity for all specimens, indicating higher crystallinity but with crystalline segments of lower molecular weight (Mw), as the exposure time to weather increases (as below appreciated in Fig. 5), which provides very brittle materials. Therefore, changes in the mechanical properties are only expected for PP2 after the second solar exposure equivalent month. This is in agreement with the mechanical test results showing high fragility of PP2 after the first two months.

### 3.4. Molecular weight distribution for PP

To gain more insights into the feasibility of using PPs in the SODIS process, the molecular weight (Mw) and molecular weight distribution (MWD) of both PP types were also measured. As PP1 displayed a stable crystallinity index, only untreated samples (week 0) were analysed (Fig. 5). Firstly, PP1 showed a lower initial molecular weight than that of PP2 (178290 vs 459770 g/mol). The higher the molecular weight, the higher the tensile strength but, the lower capability to be deformed. In this sense, PP1 is expected to be even more elastic. In addition, PP1 was also found to be a more homogeneous material due to its lower polydispersity index (PI) (7.28 vs 10.5). Regarding the evolution of the molecular weight, Fig. 5 shows a high difference between both PP materials. While PP1 remains stable since its Mw and MWD hardly varies, PP2 suffered a high degradation (chain scission, oxidation, etc.) revealed by a clear shift to lower Mw and the widening of the MWD. A possible explanation for this finding could be that shorter polypropylene chains with capability to crystallize are formed. Accounting for the FTIR spectrometry and MWD results, a PP with a small amount of UV-stabiliser added (1% by weight) is a suitable material to manufacture SODIS bottles since it can resist daily manual handling.

### 3.5. Melting and crystallinity for PP

First melting temperature ($T_{m1}$) was analysed to confirm the differences found in the PPs (Fig. 6). PP1 shows a dominating peak around 150 °C that remains unchanged with exposure weathering and is attributed to melting of isotactic polypropylene crystallites, matching well with the molecular weight distribution above mentioned [38]. In contrast, PP2 exhibited a deterioration at around 2–3 solar exposure equivalent months as $T_{m1}$ were gradually shifted towards lower temperatures, indicating some crystallization defects or smaller crystalline segments, which is indicative of possible degradation. The observed changes in the melting behavior of the weathered PP2 samples can be explained by the scissions of polymer chains, an event often reported when PP is exposed to the sun without any type of UV-Stabiliser [39,40].

### 3.6. Optical properties

Variations in the transmittance spectra due to weathering were studied for all four plastics (Fig. 7). All samples were very transparent except for the translucent PP2. For this reason, the total transmittance was assumed to be the direct transmission for PMMA, PET, and PP1, and the sum of the direct and diffuse transmittances for PP2 (details of direct and diffuse transmittance for PP2 can be found in Fig. S3).

For all the plastics, the UVA transmission was higher than for UVB. In the case of the PMMA and PP1, the UVA transmission was stable with the

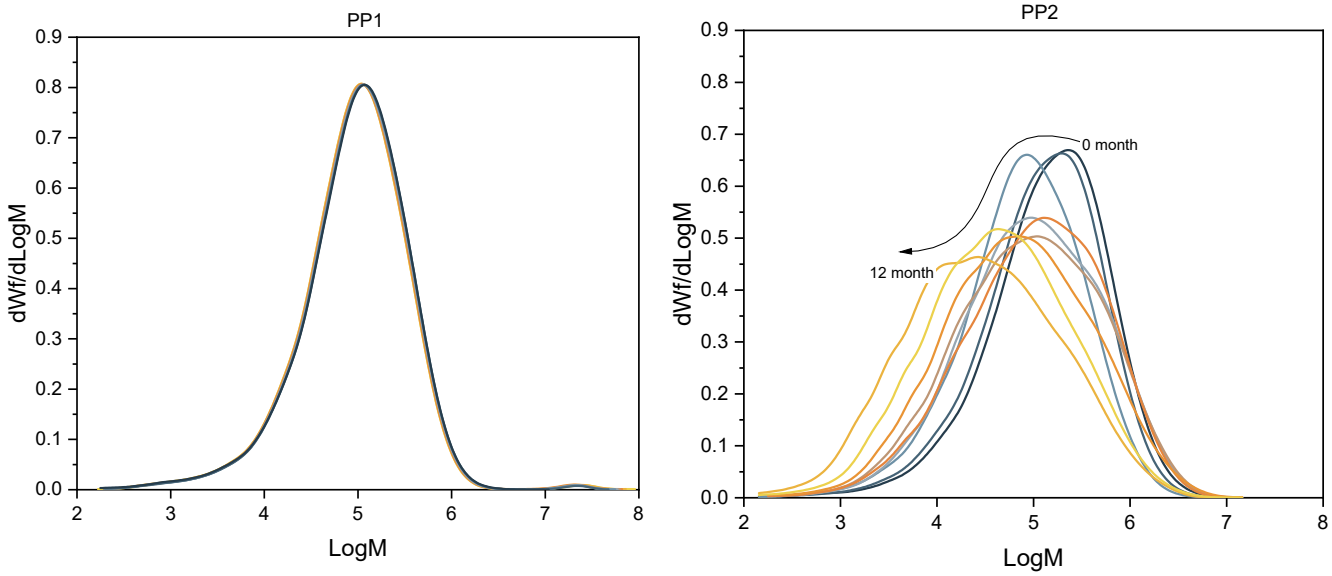


**Fig. 5.** Evolution of the MWD curves for the samples of both PPs. For PP1, the MWD curves overlap.

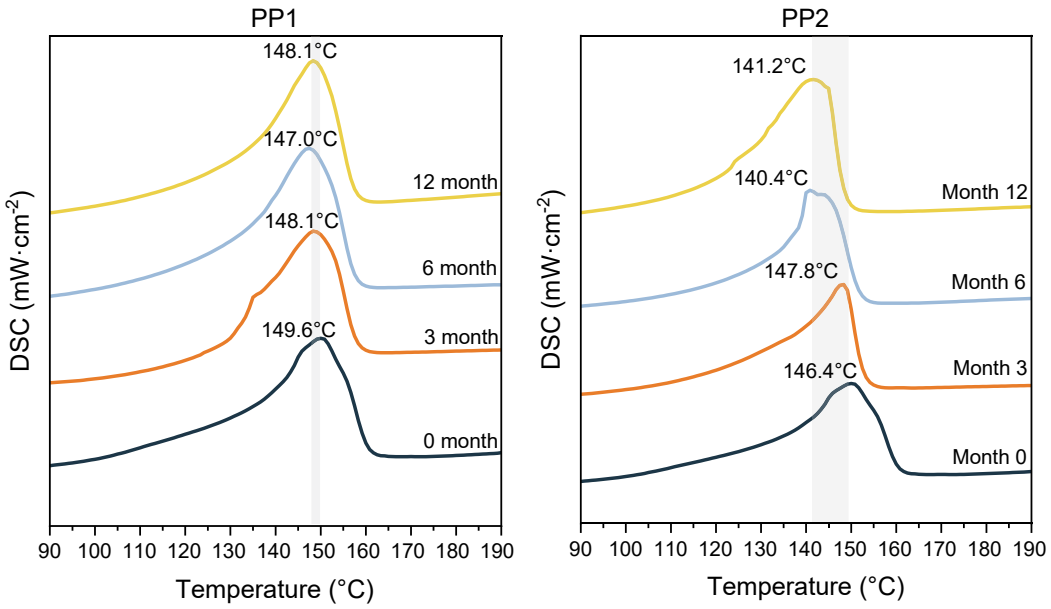


**Fig. 6.** Evolution of the DSC curves for the first melting for both PP materials.

ageing but due to different reasons. PMMA is considered a high photostability polymer, whereas PP is a poorly photostable plastic [20]. However, due to the 1% of UV-stabiliser, the UVA and UVB transmission properties remained stable during the studied period, unlike that of the PP2 (without UV stabiliser) which decreases by 15–20%. In the case of PET, it does not transmit UVB radiation (the most powerful radiation in solar photoinactivation processes) and its UV transmission also declines even 30%. These two factors make PET the least suitable material in terms of optical behaviour, and justify the search for alternative materials. The two best materials regarding their optical properties are PMMA and PP1 since both are optically photostable and transmit UVB radiation. Note that PMMA showed some degradation in UVB transmission (from 70% to 40%) during the first half of the weathering process. However, it was still the plastic that transmits the most and, after the first six equivalent months, the UVB transmission remained stable. Although the absorption of UV radiation by PMMA can lead to the formation of monomers by chain scission [20], this effect seems to be negligible.

Although only the UVB and UVA ranges of solar radiation are of interest for the inactivation of microorganisms, visible transmittance spectra have been included since they can be useful for other processes induced by visible radiation. PMMA and PET almost totally transmit the radiation in the visible range even after ageing. In contrast, PP1 and PP2 only transmit radiation around 60–70% of the visible light. The transmittance remained constant for PP1 due to the UV-stabiliser (although a slight increase in the transmittance occured due to the UV-stabiliser deterioration) but not for PP2, which decreased to 40%. Although the primary function of the UV-stabiliser is to cut the UV radiation, it seems that it also has an effect on the visible region.

### 3.7. Disinfection rates

Predictions for the *E. coli* inactivation were performed using the model found in the literature [33] (eq. (1) and (2) with values of $m = 1.1$ and $F = 1.0$). As can be observed in Fig. S4, the kinetic constants experimentally observed are far from the predictions (NRMSE: PMMA: 64.9%, PET: 76.9%, PP1: 74.4% and PP2: 81.5%). The underestimation of the predictions is probably caused by the different bacterial strains analysed, althoguh they follow a surprising behaviour: the wild *E. coli* isolated from real wastewater was inactivated faster than the culture collection laboratory strain used in the literature work. Besides that, this difference could be also produced by the inaccuracy of UVB measurement techniques (discussed later). Therefore, the kinetic model parameters have to be optimized for the specific microorganism employed in this work. Both model parameters ($m$ and $F$) were optimised using the experimental results for the untreated plastic samples (solar exposure equivalent month = 0) and took the following values: $m = 5.0$ and $F = 4.8$. Values of $m$ ranging from 1 to 9 have been reported in the literature as a function of the shoulder curvature [33,41]. The resulting fit for the inactivation profiles of *E. coli* with time can be found in Fig. S5 with a normalised root mean square error (NRMSE) of 16.6%.

Fig. 8 shows observed and predicted kinetic constants for the optimised model. It shows a good agreement for all the plastics except for PMMA (NRMSE: PMMA: 54.4%, PET: 13.6%, PP1: 17.0% and PP2: 21.3%). The reason of this discrepancy is related to the transmittance spectra, as this is the only difference between the plastics that can affect the efficacy processes. We observe in Fig. 7, PMMA retains a stable UVA trasmittance, while UVB transmittance decreases with the same trend observed for the kinetic constant (Fig. 8). However, the predictions reflect a less pronounced decrease in the inactivation kinetic constant. For this reason, the influence of the UVB radiation should be higher. This fact would lead us to expect higher changes in the kinetic constant for PMMA but not for the other plastics which transmit a lower percent of UVB radiation. One of the current research priorities in the solar disinfection field is the development of more accurate methods for quantifying the UVB portion of sunlight [4]. As is well-known, the UVB radiation is very energetic but is found in low quantities in natural or simulated solar sources. Such low intensities are very close to the error of the spectrophotometers. Therefore, small variations of spectral irradiance in the range from 280 to 300 nm could lead to significant differences in the calculation of the inactivation rates [7].

## 4. Conclusions

This work demonstrates the necessity of studying the weathering of the new plastics proposed as alternative materials for manufacturing SODIS containers. It has been proven that prolonged solar exposure can affect the efficacy of the process when the transmittance decays (worsening of the optical properties) and the containers lifetime caused by the plastic becoming brittle (worsening of the mechanical properties). However, the loss of the mechanical resistance is not crucial for selecting suitable materials if the lifetime is balanced with the costs.

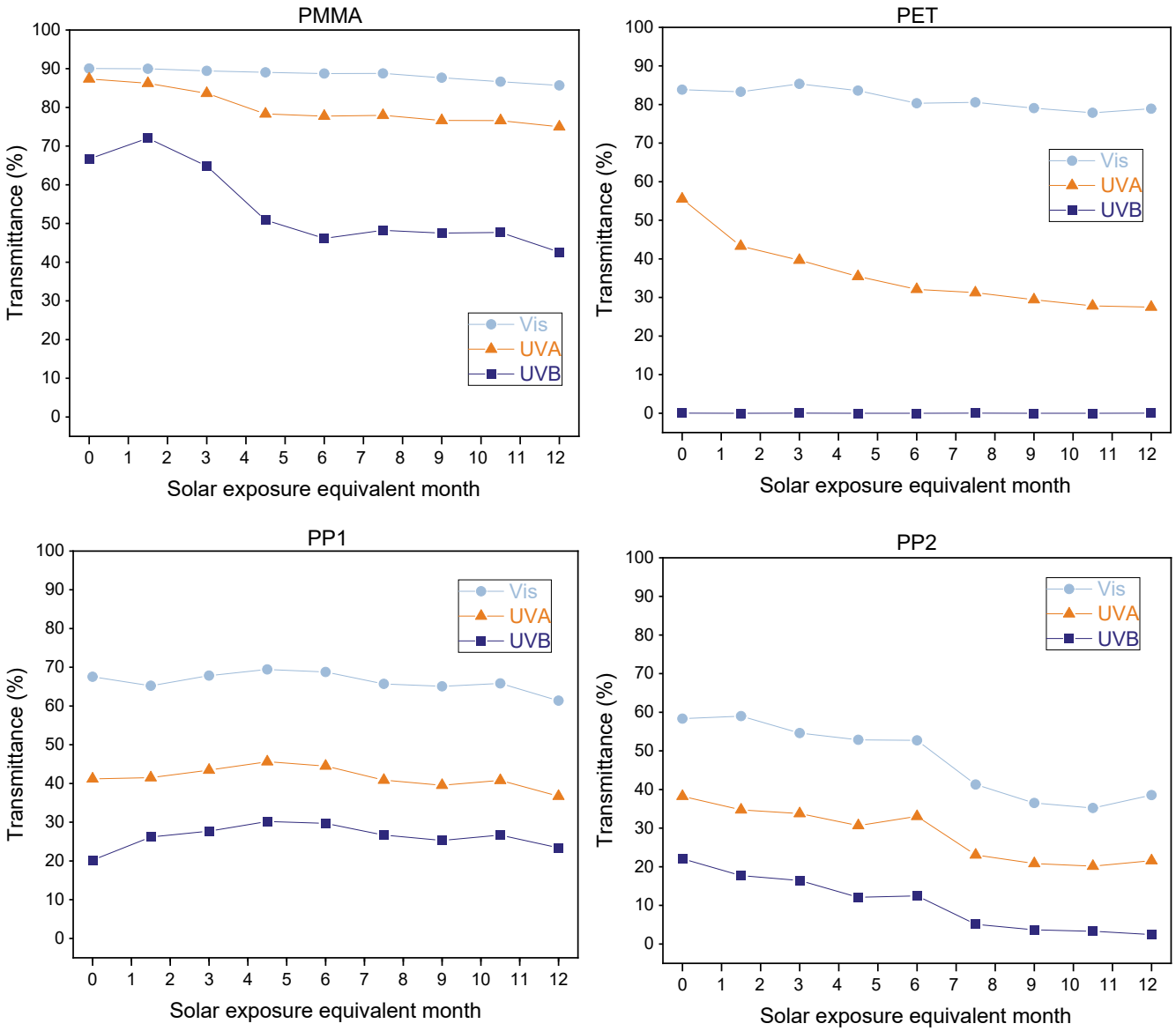


**Fig. 7.** Evolution of the transmission in the visible, UVA and UVB ranges during the ageing process. Percentage calculated as the average transmittance in the specific wavelenght range (UVB: 280–320 nm, UVA: 320–400 nm, Vis: 400–800 nm).

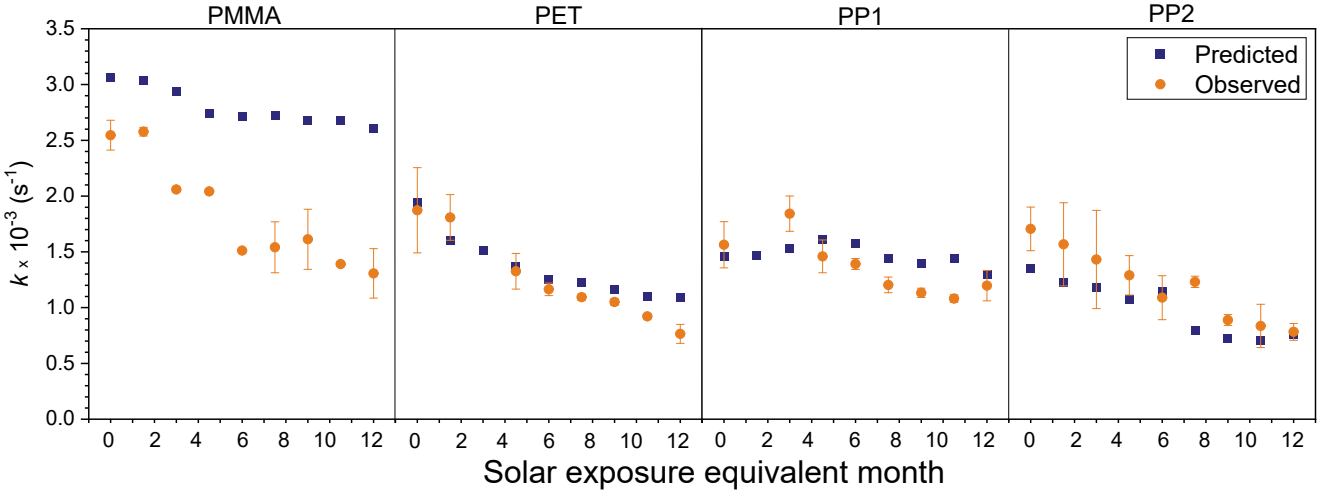


**Fig. 8.** Agreement between the observed and predicted values of the inactivation kinetic constant with the optimised kinetic model.

PMMA and PP with a 1% of UV-stabiliser were identified as excellent materials for manufacturing SODIS devices. PMMA proved to be a very photostable material with stable mechanical properties and a lifetime exceeding one year. Also, it demonstrated the best optical properties and disinfection rates. Since it is a resistant but rigid material, and is easily scratched as it is relatively soft, it is recommended for static (non-portable) SODIS devices. PP with a 1% by weight of UV-stabiliser added retained stable optical properties with high disinfection rates and good mechanical properties without signs of significant degradation after 9 months of solar exposure. Since it is an elastic and impact resistant material, it is recommended for portable SODIS devices. PET and PP without stabiliser were also analysed. Their disinfection rates were the lowest since PET does not transmit UVB radiation, and the transmittance of PP decayed due to significant ageing of the plastic. The lifetime of PET was estimated, at least, as 1 year of solar exposure while only 2 months for PP without additives. It has to be mentioned that this study corresponds to the worst case scenario, in which both sides of the SODIS container material are in contact with oxygen. Therefore, the actual lifetime of containers could be higher than that estimated here due to the protecting effect of water on the material.

In addition, a kinetic model that considers the spectral radiation distribution was optimised to estimate the solar inactivation of a wild strain of *E. coli* bacteria. The optimised model minimised the error between the predicted and the observed data below 25% for all the plastics except for the PMMA, probably caused by the inaccuracy of the current measurement techniques for UVB radiation. More accurate techniques are required for the modelling of solar processes such as solar water disinfection in which UVB radiation plays a very important role.

## Declaration of Competing Interest

The authors declare that they have no known competing financial interests or personal relationships that could have appeared to influence the work reported in this paper.

## Acknowledgements

The authors acknowledge the financial support of the European Union's Horizon 2020 research and innovation programme in the frame of the WATERSPOUTT project (GA 688928) and PANIWATER project (GA 820718), funded jointly by the European Commission and Department of Science and Technology, India. Also, the authors would like to thank Laboratorio de Tecnología de Polimeros (LATEP), located at the Rey Juan Carlos University, Spain, for the knowledge and technical support related to the polymers field. Ángela García Gil also acknowledges the Spanish Ministry of Education for her FPU grant (FPU17/04333).

## Appendix A. Supplementary data

Supplementary data to this article can be found online at https://doi.org/10.1016/j.cej.2022.134881.

## References

[1] K.G. McGuigan, R.M. Conroy, H.-J. Mosler, M. du Preez, E. Ubomba-Jaswa, P. Fernandez-Ibañez, Solar water disinfection (SODIS): A review from bench-top to roof-top, J. Hazard. Mater. 235 (2012) 29–46, https://doi.org/10.1016/j.jhazmat.2012.07.053.

[2] T. Clasen, L. Haller, D. Walker, J. Bartram, S. Cairncross, Cost-effectiveness of water quality interventions for preventing diarrhoeal disease in developing countries, J. Water Health. 5 (2007) 599–608, https://doi.org/10.2166/wh.2007.010.

[3] N. Pichel, M. Vivar, M. Fuentes, The problem of drinking water access: A review of disinfection technologies with an emphasis on solar treatment methods, Chemosphere 218 (2019) 1014–1030, https://doi.org/10.1016/j.chemosphere.2018.11.205.

[4] K.L. Nelson, A.B. Boehm, R.J. Davies-Colley, M.C. Dodd, T. Kohn, K.G. Linden, Y. Liu, P.A. Maraccini, K. McNeill, W.A. Mitch, T.H. Nguyen, K.M. Parker, R. A. Rodriguez, L.M. Sassoubre, A.I. Silverman, K.R. Wigginton, R.G. Zepp, Sunlight-mediated inactivation of health-relevant microorganisms in water: a review of mechanisms and modeling approaches, Environ. Sci. Process. Impacts. 20 (8) (2018) 1089–1122.

[5] S. Luzi, M. Tobler, F. Suter, R. Meierhofer, SODIS manual: Guidance on solar water disinfection, EAWAG, Switzerland, 2016.

[6] Á. García-Gil, C. Pablos, R.A. García-Muñoz, K.G. McGuigan, J. Marugán, Material selection and prediction of solar irradiance in plastic devices for application of solar water disinfection (SODIS) to inactivate viruses, bacteria and protozoa, Sci. Total Environ. 730 (2020) 139126, https://doi.org/10.1016/j.scitotenv.2020.139126.

[7] Á. García-Gil, A. Martínez, M.I. Polo-López, J. Marugán, Kinetic modeling of the synergistic thermal and spectral actions on the inactivation of viruses in water by sunlight, Water Res. 183 (2020) 116074, https://doi.org/10.1016/j.watres.2020.116074.

[8] Á. García-Gil, M.J. Abeledo-Lameiro, H. Gómez-Couso, J. Marugán, Kinetic modeling of the synergistic thermal and spectral actions on the inactivation of Cryptosporidium parvum in water by sunlight, Water Res. 185 (2020) 116226, https://doi.org/10.1016/j.watres.2020.116226.

[9] M.B. Fisher, M. Iriarte, K.L. Nelson, Solar water disinfection (SODIS) of *Escherichia coli, Enterococcus spp.*, and MS2 coliphage: Effects of additives and alternative container materials, Water Res. 46 (6) (2012) 1745–1754, https://doi.org/10.1016/j.watres.2011.12.048.

[10] K. Lawrie, A. Mills, M. Figueredo-Fernández, S. Gutiérrez-Alfaro, M. Manzano, M. Saladin, UV dosimetry for solar water disinfection (SODIS) carried out in different plastic bottles and bags, Sensors Actuators B Chem. 208 (2015) 608–615, https://doi.org/10.1016/J.SNB.2014.11.031.

[11] E. Ubomba-Jaswa, P. Fernández-Ibáñez, C. Navntoft, M.I. Polo-López, K. G. McGuigan, Investigating the microbial inactivation efficiency of a 25 L batch solar disinfection (SODIS) reactor enhanced with a compound parabolic collector (CPC) for household use, J Chem Technol Biotechnol. 85 (8) (2010) 1028–1037, https://doi.org/10.1002/jctb.2398.

[12] B. Reyneke, T. Ndlovu, M.B. Vincent, A. Martínez-García, M.I. Polo-López, P. Fernández-Ibáñez, G. Ferrero, S. Khan, K.G. McGuigan, W. Khan, Validation of large-volume batch solar reactors for the treatment of rainwater in field trials in sub-Saharan Africa, Sci. Total Environ. 717 (2020) 137223, https://doi.org/10.1016/j.scitotenv.2020.137223.

[13] A. Martínez-García, I. Oller, M. Vincent, V. Rubiolo, J.K. Asiimwe, C. Muyanja, K. G. McGuigan, P. Fernández-Ibáñez, M. Inmaculada Polo-López, Inmaculada Polo-López, Meeting daily drinking water needs for communities in Sub-Saharan Africa using solar reactors for harvested rainwater, Chem. Eng. J. 428 (2022) 132494, https://doi.org/10.1016/j.cej.2021.132494.

[14] S. Rufener, D. Mäusezahl, H.-J. Mosler, R. Weingartner, Quality of drinking-water at source and point-of-consumption-drinking cup as a high potential recontamination risk: a field study in Bolivia, J. Health. Popul. Nutr. 28 (2010) 34–41, https://doi.org/10.3329/jhpn.v28i1.4521.

[15] H.G. Fagan, K.S. Linnane, K.G. McGuigan, A. Rugamayo, Water is life – Progress to secure water provision in rural Uganda, Practical Action Publishing, Rugby, UK, 2015.

[16] A. Martínez-García, M. Vincent, V. Rubiolo, M. Domingos, M.C. Canela, I. Oller, P. Fernández-Ibáñez, M.I. Polo-López, Assessment of a pilot solar V-trough reactor for solar water disinfection, Chem. Eng. J. 399 (2020) 125719, https://doi.org/10.1016/j.cej.2020.125719.

[17] K.T. Gillen, M. Celina, Predicting polymer degradation and mechanical property changes for bombined radiation-thermal aging environments, Rubber Chem. Technol. 91 (2017) 27–63, https://doi.org/10.5254/rct.18.81679.

[18] J.R. Martin, R.J. Gardner, Effect of long term humid aging on plastics, Polym. Eng. Sci. 21 (9) (1981) 557–565, https://doi.org/10.1002/pen.760210908.

[19] J.R. White, Polymer ageing: physics, chemistry or engineering? Time to reflect, Comptes Rendus Chim. 9 (11-12) (2006) 1396–1408, https://doi.org/10.1016/j.crci.2006.07.008.

[20] B. Rånby, Basic reactions in the photodegradation of some important polymers, J. Macromol. Sci. Part A, Pure Appl. Chem. 30 (9-10) (1993) 583–594, https://doi.org/10.1080/10601329308021247.

[21] K. Kircher, Chemical reactions in plastics processing, C. Hanser, Munich, 1987.

[22] Á. García-Gil, R.A. García-Muñoz, K.G. McGuigan, J. Marugán, Solar Water Disinfection to produce safe drinking water: A review of parameters, enhancements, and modelling approaches to make SODIS faster and safer, Molecules 26 (2021) 3431, https://doi.org/10.3390/molecules26113431.

[23] Á. García-Gil, R. Valverde, R.A. García-Muñoz, K.G. McGuigan, J. Marugán, Solar Water Disinfection in high-volume containers: Are naturally occurring substances attenuating factors of radiation? Chem. Eng. J. 399 (2020) 125852, https://doi.org/10.1016/j.cej.2020.125852.

[24] M.I. Polo-López, A. Martínez-García, M.J. Abeledo-Lameiro, H. H. Gómez-Couso, E. E. Ares-Mazás, A. Reboredo-Fernández, T.D. Morse, L. Buck, K. Lungu, K. G. McGuigan, P. Fernández-Ibáñez, Microbiological evaluation of 5 L- and 20 L-transparent polypropylene buckets for Solar Water Disinfection (SODIS), Molecules 24 (11) (2019) 2193, https://doi.org/10.3390/molecules24112193.

[25] T. Morse, K. Luwe, K. Lungu, L. Chiwaula, W. Mulwafu, L. Buck, R. Harlow, G. H. Fagan, K. McGuigan, A transdisciplinary methodology for introducing Solar Water Disinfection to rural communities in Malawi—Formative research findings, Integr. Environ. Assess. Manag. 16 (2020) 871–884, https://doi.org/10.1002/ieam.4249.

[26] TotalEnergies, Technical Data of PPR 3221, (n.d.). https://polymers.totalenergies.com/ppr-3221 (accessed December 1, 2021).

[27] Atlas Material Testing Technology LLC®, Instruction Manual. Ci3000+/Ci4000/Ci5000 Xenon Arc Weather-Ometer, in: Chicago, 2005.
[28] J. Moreno-SanSegundo, S. Giannakis, S. Samoili, G. Farinelli, K.G. McGuigan, C. Pulgarín, J. Marugán, SODIS potential: A novel parameter to assess the suitability of solar water disinfection worldwide, SODIS potential: a novel parameter to assess the suitability of solar water disinfection worldwide 419 (2021) 129889, https://doi.org/10.1016/j.cej.2021.129889.
[29] O. Kuvshinnikova, G. Boven, J.E. Pickett, Weathering of aromatic engineering thermoplastics: Comparison of outdoor and xenon arc exposures, Polym. Degrad. Stab. 160 (2019) 177–194, https://doi.org/10.1016/j.polymdegradstab.2018.12.011.
[30] I. Prabowo, J. Nur Pratama, M. Chalid, The effect of modified ijuk fibers to crystallinity of polypropylene composite, IOP Conf, Ser. Mater. Sci. Eng. 223 (2017) 012020.
[31] K.K. Philippe, R. Timmers, R. van Grieken, J. Marugan, Photocatalytic disinfection and removal of emerging pollutants from effluents of biological wastewater treatments, using a newly developed large-scale solar simulator, Ind. Eng. Chem. Res. 55 (11) (2016) 2952–2958, https://doi.org/10.1021/acs.iecr.5b04927.
[32] W. Harm, Biological effects of ultraviolet radiation, University Press, United Kingdom, 1980.
[33] A.I. Silverman, K.L. Nelson, Modeling the endogenous sunlight inactivation rates of laboratory strain and Wastewater *E. coli* and *enterococci* using biological weighting functions, Environ. Sci. Technol. 50 (22) (2016) 12292–12301, https://doi.org/10.1021/acs.est.6b03721.
[34] R. Frischknecht, N. Jungbluth, H.-J. Althaus, G. Doka, R. Dones, T. Heck, S. Hellweg, R. Hischier, T. Nemecek, G. Rebitzer, M. Spielmann, The ecoinvent database: Overview and methodological framework, Int. J. Life Cycle Assess. 10 (2005) 3–9, https://doi.org/10.1065/lca2004.10.181.1.
[35] K. Rajakumar, V. Sarasvathy, A. Thamarai Chelvan, R. Chitra, C.T. Vijayakumar, Natural weathering studies of polypropylene, J. Polym. Environ. 17 (3) (2009) 191–202, https://doi.org/10.1007/s10924-009-0138-7.
[36] J. Xiong, X. Liao, J. Zhu, Z. An, Q. Yang, Y. Huang, G. Li, Natural weathering mechanism of isotatic polypropylene under different outdoor climates in China, Polym. Degrad. Stab. 146 (2017) 212–222, https://doi.org/10.1016/j.polymdegradstab.2017.10.012.
[37] PlasticEurope, Eco-profiles and environmental declarations - LCI methodology and PCR for uncompounded polymer resins and reactive polymer precursor. v. 3.0, (2012). www.plasticeurope.org.
[38] A. Fernández, M.T. Expósito, B. Peña, R. Berger, J. Shu, R. Graf, H.W. Spiess, R. A. García-Muñoz, Molecular structure and local dynamic in impact polypropylene copolymers studied by preparative TREF, solid state NMR spectroscopy, and SFM microscopy, Polymer (Guildf). 61 (2015) 87–98, https://doi.org/10.1016/j.polymer.2015.01.079.
[39] A. Niemczyk, K. Dziubek, M. Grzymek, K. Czaja, Accelerated laboratory weathering of polypropylene composites filled with synthetic silicon-based compounds, Polym. Degrad. Stab. 161 (2019) 30–38, https://doi.org/10.1016/j.polymdegradstab.2019.01.005.
[40] L. Marsich, A. Ferluga, L. Cozzarini, M. Caniato, O. Sbaizero, C. Schmid, The effect of artificial weathering on PP coextruded tape and laminate, Compos. Part A Appl. Sci. Manuf. 95 (2017) 370–376, https://doi.org/10.1016/j.compositesa.2017.01.016.
[41] L.W. Sinton, C.H. Hall, P.A. Lynch, R.J. Davies-Colley, Sunlight inactivation of fecal indicator bacteria and bacteriophages from waste stabilization pond effluent in fresh and saline waters, Appl. Environ. Microbiol. 68 (3) (2002) 1122–1131, https://doi.org/10.1128/AEM.68.3.1122-1131.2002.